



# Particle Correlations from ALICE: Latest Results

Andrew M. Adare (for the ALICE Collaboration)<sup>1</sup>

*Yale University, New Haven, CT, USA*

## Abstract

The correlation between pairs or triplets of particles in relative angle and momentum provides a valuable means of accessing the physics of particle production in heavy ion collisions. A selection of recent results from two and three particle correlations measured by the ALICE experiment are presented, and some brief interpretations of their implications are offered.

## 1. Introduction

The measurement of angular distributions from two and three particle correlations has proven to be an effective technique for studying the modification of particle production in heavy ion collisions, particularly when used in comparison to expectations from proton-proton collisions. The correlation technique involves constructing a density of pair angles in relative azimuth ( $\Delta\varphi = \varphi_t - \varphi_a$ ) or pseudorapidity ( $\Delta\eta = \eta_t - \eta_a$ ), where  $t$  and  $a$  denote trigger particles with momentum  $p_T^t$  and associated particles at momentum  $p_T^a$ .

Peaks in a correlation function indicate a relatively high probability for particle coincidence in a particular region of phase space for the pair; accordingly, depletions indicate a lower probability. Interpretation of such distributions allows inference to properties of the hot, dense quark-gluon plasma phase of nuclear matter produced in ultrarelativistic nuclear collisions. Of particular interest is the modification of the shape and yield of particle pair distributions, which shed light on processes associated with initial-state physics and hydrodynamic evolution, as well as jet fragmentation and hadronic interactions occurring in the final state.

## 2. Baryon to meson ratios

We begin with an investigation of the intriguing “Baryon anomaly” observed previously at RHIC [1] and more recently at the LHC [2]. Within a  $p_T$  range of approximately 2–5 GeV/ $c$ , the ratio of baryons to mesons is enhanced by up to a factor of four in central Pb–Pb compared to pp collisions. This phenomenon is studied in two-particle correlations, where the conditional yield of associated baryons (specifically  $p, \bar{p}$ ) and mesons ( $\pi^\pm$ ) is measured on the near side (i.e.  $-\Delta\varphi < 0.5$ ) for a “peak” region ( $\Delta\varphi, \Delta\eta$  near 0, 0) and in “bulk” regions ( $|\Delta\eta| > 0.6$ ). See figure 1, left.

For this analysis, the trigger particles consist of non-identified charged hadrons in  $5 < p_T^t < 10$  GeV/ $c$ . The associated pions and protons were identified using measured energy loss in the

<sup>1</sup>A list of members of the ALICE Collaboration and acknowledgements can be found at the end of this issue.

© CERN for the benefit of the ALICE Collaboration. Open access under [CC BY-NC-ND license](https://creativecommons.org/licenses/by-nc-nd/4.0/).

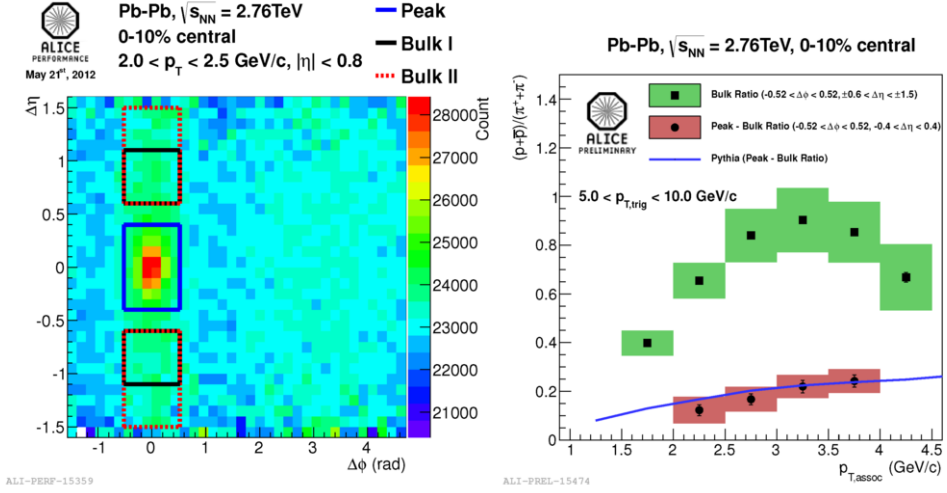


Figure 1: (Left) Example of a particle pair distribution in  $(\Delta\phi, \Delta\eta)$  showing the “peak” and “bulk” angular windows. (Right) ratio of proton/pion spectra as a function of  $p_T^a$  for the peak and bulk regions, including  $p/\pi$  from PYTHIA.

ALICE time projection chamber (TPC) and flight time from the ALICE time-of-flight detector. The right side of figure 1 shows the ratio of proton/pion spectra in the two angular regions as a function of  $p_T^a$ . It is found that  $p/\pi$  in the near-side (bulk-subtracted) peak region is consistent with the expectation from proton-proton collisions, as estimated by a default tune of PYTHIA v6.4.21 [3], while  $p/\pi$  is strongly enhanced in the “bulk” region. This suggests firstly that there is no significant medium-induced modification of jet particle ratios, and secondly that the aforementioned baryon enhancement in heavy ion collisions is a result of bulk processes and not jet fragmentation.

### 3. Near-side peak studies

A number of observables, such as the nuclear modification factor  $R_{AA}$  (for single particles) and  $I_{AA}$  (for particle pairs), have suggested a significant medium-induced energy loss of hard-scattered partons. The latter is defined as

$$I_{AA} = \frac{Y_{AA}}{Y_{pp}}, \quad Y = \int d\Delta\phi \frac{1}{N_{trig}} \frac{dN_{pair}}{d\Delta\phi}. \quad (1)$$

From recent analyses of reconstructed jets [4], the energy loss initially indicated by observables such as  $I_{AA}$  has been interpreted as large-angle soft radiation, with weakly modified remnant jets. This interpretation is studied further here by examining the width and eccentricity of near-side peaks in dihadron correlations. The large combinatoric non-jet component of the dihadron correlations is estimated from the large- $\Delta\eta$  component (visible in figure 2, upper left), and is subtracted from the inclusive sample, leaving a distribution such as the example in figure 2 (lower left). The resulting peaks follow clear trends with  $p_T$  and collision centrality (figure 2, right). First, the widths in  $\Delta\eta$  are greater than those in  $\Delta\phi$ . The widths decrease as the particle  $p_T$  rises.

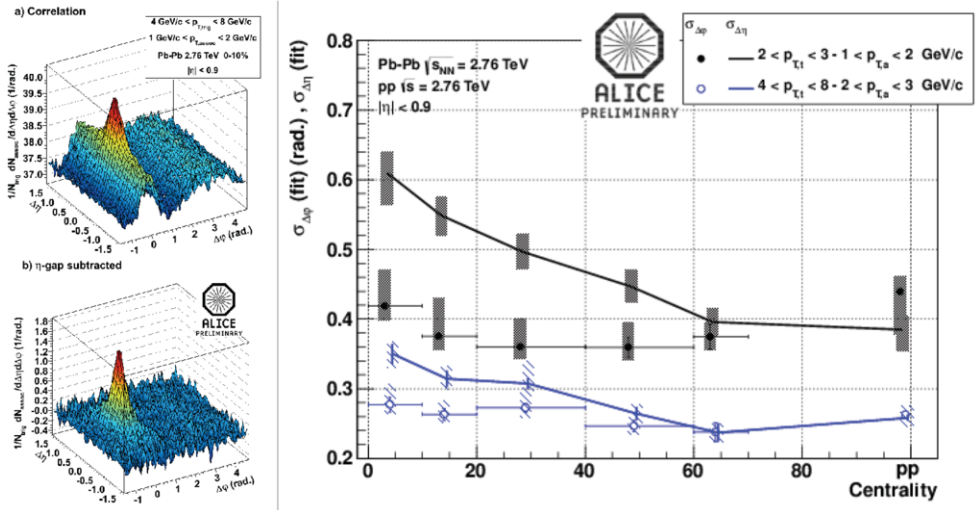


Figure 2: Left: example of an angular distribution of charged-particle pairs including all correlation sources (top), and with large- $\Delta\eta$  correlations subtracted, such that jet-like correlation is the dominant remaining component (bottom). Right: widths from Gaussian peak fits in  $\Delta\phi$  (points) and  $\Delta\eta$  (lines) for lower- $p_T$  pairs (upper curves) and higher- $p_T$  pairs (lower curves).

Narrowing is also visible in both coordinates as collisions become more peripheral, although this trend is considerably weaker in  $\Delta\phi$  than in  $\Delta\eta$ .

One explanation for the system-size dependence of the peak width is longitudinal hydrodynamic flow [5], which can deform a jet produced with an initially conical profile.

In addition to analysis of peak widths, modification of the near-side yields has also been measured. The estimated non-jet background has been estimated from conditional yields away from the peak as described in [6] and is subtracted. The result is shown in figure 3.

An enhancement of about 20-50% is observed in central Pb-Pb compared to the pp reference, while almost no enhancement is found in peripheral collisions. Although not shown here,  $I_{AA}$  was also measured as a function of  $\Delta\eta$ . It was found that the yield enhancement in central collisions occurs primarily at small  $\Delta\eta$  in the vicinity of the near-side peak. Possible explanations for this observation are presented in [6].

#### 4. Charge-dependent correlations

Charge balance functions, defined for  $\Delta\eta$  as

$$B(\Delta\eta) = \frac{1}{2} \left\{ \frac{N_{+-}(\Delta\eta) - N_{++}(\Delta\eta)}{N_+} + \frac{N_{-+}(\Delta\eta) - N_{--}(\Delta\eta)}{N_-} \right\} \quad (2)$$

and similarly for  $\Delta\eta \rightarrow \Delta\phi$ , provide a valuable tool to study collective motion, charge separation at the freeze-out stage, and the time of hadronization.

Two different samples are provided as references for the charge balance measurements. First, a shuffled-event sample is produced by randomizing the charges of tracks within each event, so

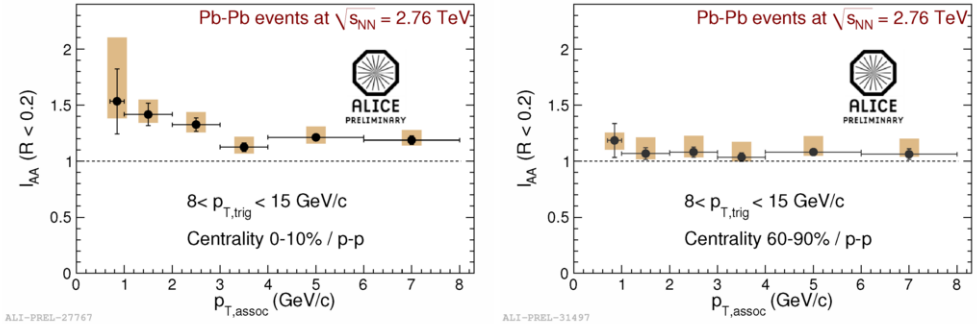


Figure 3: Near-side  $I_{AA}$  vs. associated particle  $p_T$  for 8-15 GeV/c trigger particles in central collisions (left) and peripheral collisions (right).

that charge-momentum correlations are removed. Secondly, a mixed-event sample is generated by correlating tracks between events, where all correlations of physical origin are removed, and only acceptance effects are present.

The balance functions for the three samples are shown in figure 4 (for  $\Delta\eta$ ) and figure 5 (for  $\Delta\varphi$ ). In both coordinates, the balance function falls to zero with increasing pair separation, becoming narrower in more central collisions. This focusing effect is consistent with strong radial flow and a delay in the creation of charges due to a long lifetime of the thermalized medium, as explained in [7].

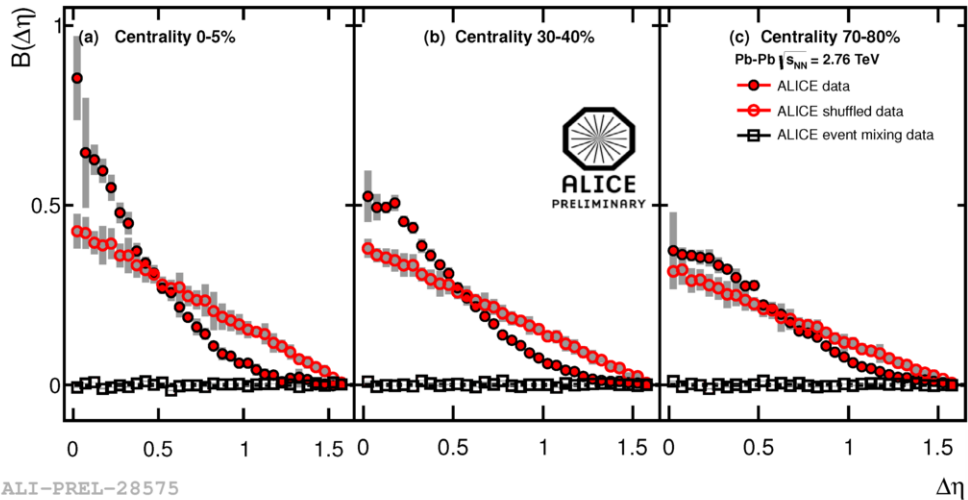


Figure 4: Charge balance function (eq. 2) for central (left), mid-central (center) and peripheral (right) collisions.

In addition to charge balance functions, number density ( $R_2$ ) and transverse momentum

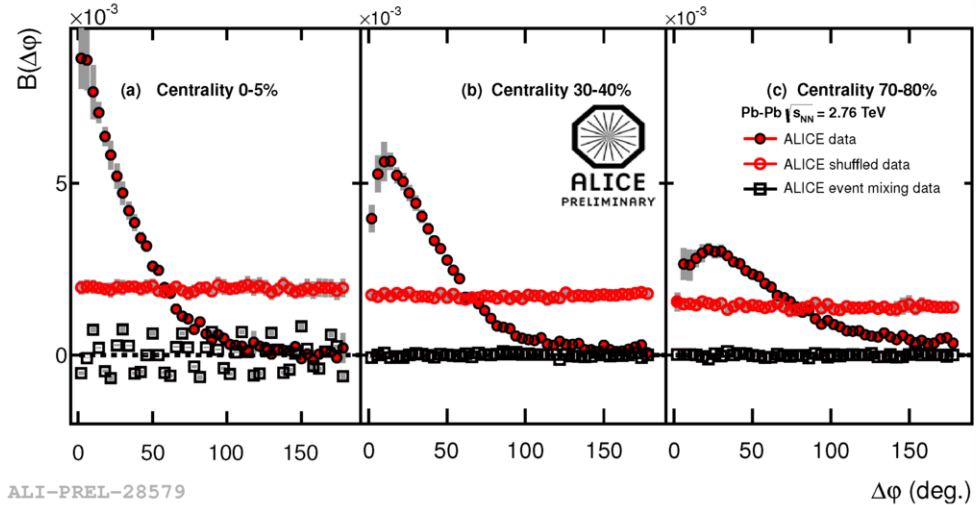


Figure 5: Balance function similar to figure 4, but measured vs.  $\Delta\phi$  instead of  $\Delta\eta$ .

$(\Delta p_T - \Delta p_T)$  correlations were also measured in various  $\Delta\eta$  intervals. The latter are omitted from these proceedings for lack of space. Fourier harmonics were extracted from fits to the azimuthal distributions. Correlations at large  $\Delta\eta$  exclude the near-side peak from jet fragmentation and other nonflow sources. The general trends were as follows: the second through fourth harmonics extracted from  $R_2$  were found to be consistent with those obtained via more traditional techniques such as the event-plane method. An example is shown in the left side of figure 6. The  $v_2$ - $v_4$  coefficients also followed a pair harmonic factorization into single-particle harmonics, in the sense described in [8]. The harmonics from the three charge combinations ( $++$ ,  $+ -$ , and  $--$ ) were found to agree with one another.

The first harmonic, however, did not exhibit such trends (figure 6, right). There, opposite-sign pairs are seen to have a significantly different value than like-sign pairs. It is likely that  $v_1$  behaves differently than the higher harmonics due to momentum and charge conservation effects.

## 5. Three particle correlations

Three particle correlations have also been measured in a variety of  $p_T$  and centrality ranges. For this analysis, two different associated particles are paired with a trigger particle, leading to a two-dimensional  $\Delta\phi_{12}, \Delta\phi_{13}$  distribution proportional to the probability to obtain two associated particles with the trigger. An example for the 5% most central collisions for particles at intermediate  $p_T$  ( $3 < p_T^t < 4$ ,  $1 < p_T^a < 2$  GeV/c) is shown in figure 7.

The pattern observed in Pb-Pb data is similar to the result of a simulation that incorporates only hydrodynamics without any kind of jet fragmentation. This observation is consistent with previous two-particle measurements from the ALICE collaboration that have indicated an overwhelming dominance of hydrodynamic flow to the azimuthal anisotropy [9]. Thus any non-flow

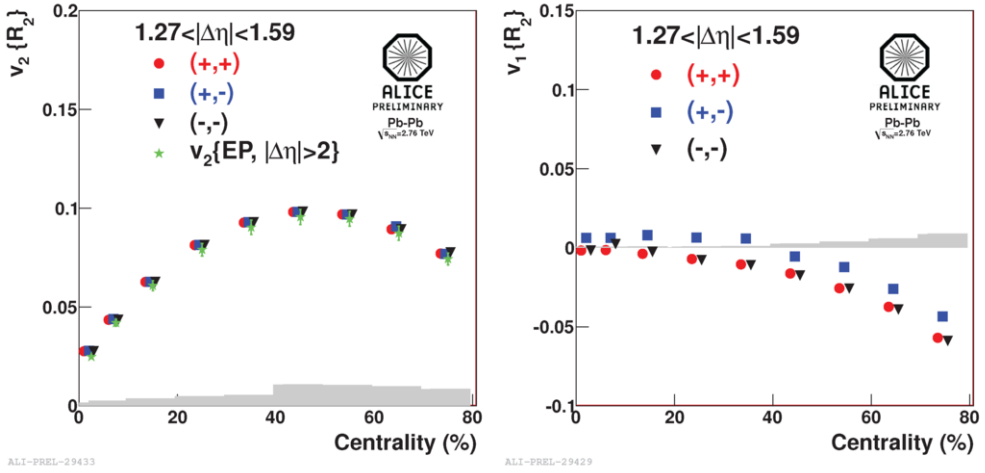


Figure 6: Examples of Fourier harmonics extracted from fits to number density  $R_2$  correlations. Left:  $v_2\{R_2\}$ . Right:  $v_1\{R_2\}$ .

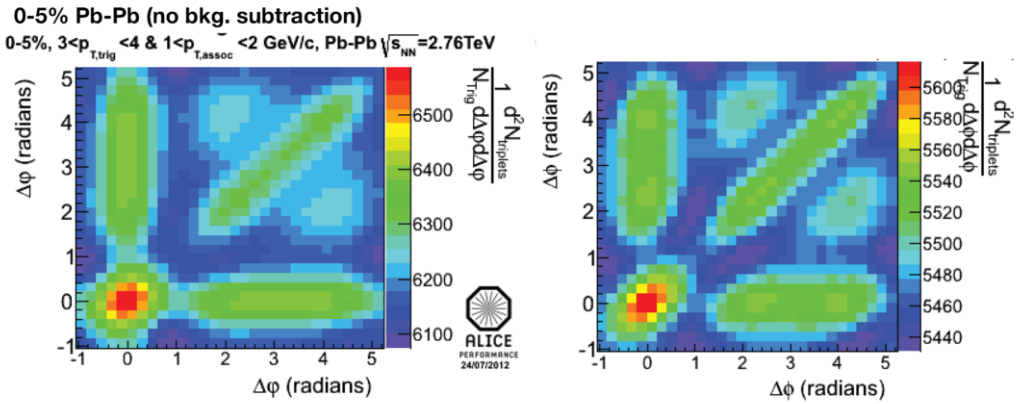


Figure 7: Azimuthal distributions  $\Delta\phi_{12}, \Delta\phi_{13}$  for particle triplets with a trigger particle at  $\phi_1$  and associated particles at  $\phi_{2,3}$ . Left: 0-5% central Pb-Pb data, Right: result of flow-only simulation at the same centrality.

signal must be comparatively small, although attempts are underway to isolate such a contribution if present [10].

## 6. Femtoscopic correlations

Continuing the analysis of global event properties from two-particle correlations, the femtoscopic radii  $R_{inv}$  from Bose-Einstein correlations are shown in figure 8 for pions, kaons, and protons as a function of transverse mass  $m_T = \sqrt{p_T^2 + m^2}$ . Each family of particles with a common mass follows an approximate inverse-power trend in  $m_T$  up to 1.6 GeV/ $c^2$ , if a kinematic normalization factor is applied. This approximate  $m_T$  scaling is expected if the space-momentum correlation for these species is induced by hydrodynamic flow [11].

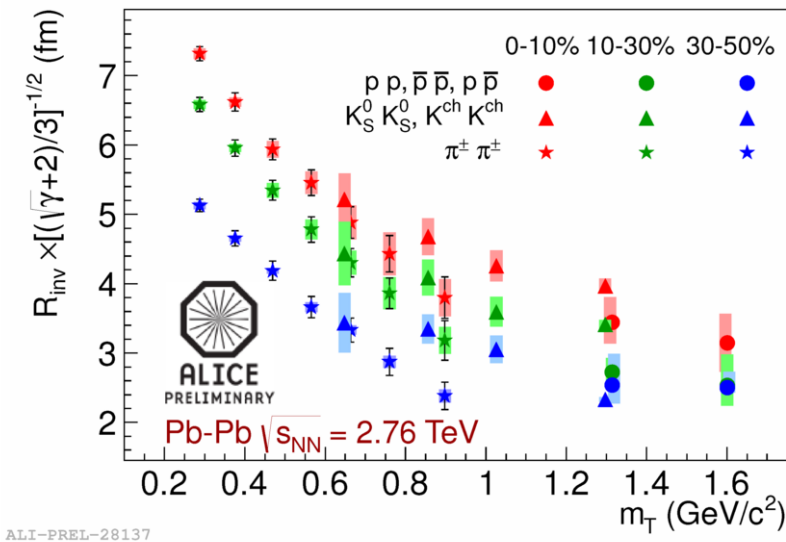


Figure 8: Femtoscopic radius  $R_{inv}$  for pion ( $\star$ ), kaon ( $\blacktriangle$ ), and proton ( $\bullet$ ) pairs in three different centrality classes.

Baryon-antibaryon ( $B\bar{B}$ ) correlation functions have been measured as a function of relative momentum and are shown in figure 9 for protons (left) and  $\Lambda$ s (right).

For the  $p\bar{p}$  correlations, an enhancement in the femtoscopic correlation function  $C$  is observed at the lowest relative momenta due to well-known Coulomb effects, but for both species a broad depletion is observed. This has been explained as consistent with final-state ( $B\bar{B}$ ) annihilation. Such an effect, thought to occur during the hadronic rescattering phase of heavy ion collisions, has also been invoked to explain the observed reduction in proton yields relative to expectations from hydrodynamic models.

Thus, these measurements support the mechanism of final-state ( $B\bar{B}$ ) pair annihilation, and serve as the beginnings of precise interaction cross-section measurements for several rare ( $B\bar{B}$ ) pair types, which are useful in their own right, as well as providing quantitative inputs for hadronic cascade models such as URQMD.

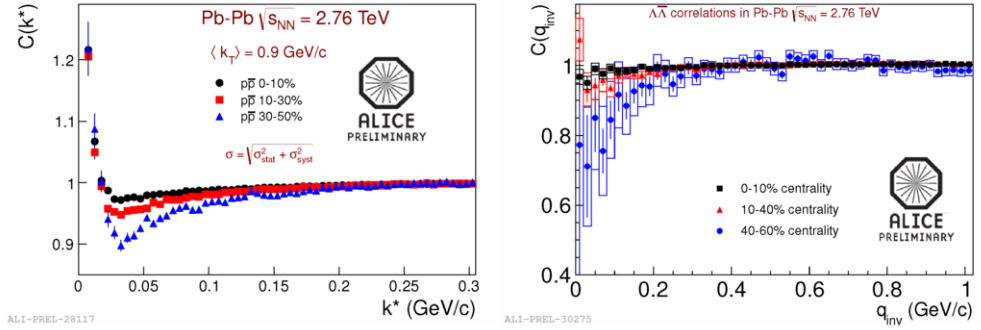


Figure 9: Baryon-antibaryon correlation functions as a function of relative momentum for  $p\bar{p}$  pairs (left) and  $\Lambda\bar{\Lambda}$  pairs (right).

## 7. Summary

The results presented here provide new insights into medium modification, both qualitatively and quantitatively, but have generally served to support the most common current interpretations of existing results.

From correlations involving identified particles, it appears that the baryon enhancement arises from collective physics rather than jet fragmentation. The similarity in particle composition between  $Pb-Pb$  and proton-proton collisions suggests that jet fragmentation occurs in vacuum rather than inside the medium. In addition,  $(B\bar{B})$  correlations suggest that pair annihilation is a significant effect in the final state.

At low to intermediate  $p_T$ , the data suggest that hydrodynamic flow is a dominant cause of anisotropy. Three-particle correlations in central Pb-Pb data are consistent with flow-only simulations. Recent transverse momentum and number density correlations, omitted from these proceedings for lack of space, have also supported the picture of flow-dominated correlations.

Analyses of the shape and yield of the near-side correlation peak indicate significant medium modification, in the form of longitudinal broadening effect observed in increasingly central collisions, and an enhancement in associated yields compared to proton-proton collisions.

The balance of charges is increasingly focused to narrower relative pseudorapidity with more central collisions, suggesting strong radial flow and a long lifetime of the quark-gluon plasma phase.

## References

- [1] Brodsky, S. and Sickles, A. Physics Letters B Volume 668, Issue 2, 2 October 2008, Pages 111115
- [2] Ortiz Velasquez, A. Proceedings, this volume.
- [3] M. Veldhoen, arXiv:1207.7195v2.
- [4] The ATLAS collaboration. arXiv:1208.1967v1
- [5] Armesto, N., Salgado, C., and Wiedemann, U. Phys. Rev. Lett. 93, 242301 (2004).
- [6] Krizek, F. Proceedings, this volume.
- [7] Weber, M. Proceedings, this volume.
- [8] ALICE Collaboration. Physics Letters B 708, 249 (2012).
- [9] ALICE Collaboration. PRL 107, 032301 (2011).
- [10] Ulery, J. Proceedings, this volume.
- [11] Szymanski, M. Proceedings, this volume.